2017

A comparison study of decomposition mechanisms of single-cation and double-cations (Li, Al) ammine borohydrides

Xiaowei Chen
Jimei University, Fudan University, chenx@nju.edu.cn

Renquan Li
Jimei University

Guanglin Xia
University of Wollongong, guanglin@uow.edu.au

Hongsheng He
Jimei University

Weidong Zou
Jimei University

See next page for additional authors

Publication Details

Chen, X., Li, R., Xia, G., He, H., Zou, W. & Yu, X. (2017). A comparison study of decomposition mechanisms of single-cation and double-cations (Li, Al) ammine borohydrides. International Journal of Hydrogen Energy, 42 (39), 24861-24867.

A comparison study of decomposition mechanisms of single-cation and double-cations (Li, Al) ammine borohydrides

Abstract
The decomposition mechanisms of [Li(NH 3)][BH 4], [Al(NH 3) 6][BH 4] 3 and [Al(NH 3) 6][Li 2 (BH 4) 5] were investigated using Density functional theory (DFT) calculation. The calculated results show that [Li(NH 3)][BH 4] has low NH 3 vacancy formation energy and diffusion barrier, therefore ammonia would easily release at relatively low temperature. Both [Al(NH 3) 6][BH 4] 3 and [Al(NH 3) 6][Li 2 (BH 4) 5] show relatively high NH 3 vacancy formation energies and diffusion barriers, which avoid ammonia release at low temperature. In addition, the calculated H 2 formation energy barriers, i.e., [Al(NH 3) 6][Li 2 (BH 4) 5] < [Al(NH 3) 6][BH 4] 3 < [Li(NH 3)][BH 4], are in agreement with the tendency of dehydrogenation temperatures determined experimentally. The incorporation of [BH 4] - into [Al(NH 3) 6][BH 4] 3 play an important role in decreasing the dehydrogenation temperature and improving the hydrogen purity of [Al(NH 3) 6][Li 2 (BH 4) 5].

Disciplines
Engineering | Physical Sciences and Mathematics

Publication Details
Chen, X., Li, R., Xia, G., He, H., Zou, W. & Yu, X. (2017). A comparison study of decomposition mechanisms of single-cation and double-cations (Li, Al) ammine borohydrides. International Journal of Hydrogen Energy, 42 (39), 24861-24867.

Authors
Xiaowei Chen, Renquan Li, Guanglin Xia, Hongsheng He, Weidong Zou, and Xuebin Yu

A comparison study of decomposition mechanisms of single-cation and double-cations (Li, Al) ammine borohydrides

Xiaowei Chen[ab], Renquan Li[a], Guanglin Xia[c], Hongsheng He[a], Weidong Zou[a*], Xuebin Yu[b*]

[a] Department of Physics, School of Science, Jimei University, Xiamen, 361021, China

[b] Department of Materials Science, Fudan University, Shanghai 200433, China

[c]Institute for Superconducting and Electronic Materials, University of Wollongong, North Wollon gong, NSW, Australia

[*] To whom correspondence should be addressed.

E-mail: phyzwd@jmu.edu.cn

yuxuebin@fudan.edu.cn

ABSTRACT

The decomposition mechanisms of $[Li(NH_3)][BH_4]$, $[Al(NH_3)_6][BH_4]_3$ and $[Al(NH_3)_6][Li_2(BH_4)_5]$ were investigated using Density functional theory (DFT) calculation. The calculated results show that $[Li(NH_3)][BH_4]$ has low NH_3 vacancy formation energy and diffusion barrier, therefore ammonia would easily release at relatively low temperature. Both $[Al(NH_3)_6][BH_4]_3$ and $[Al(NH_3)_6][Li_2(BH_4)_5]$ show relatively high NH_3 vacancy formation energies and diffusion barriers, which avoid ammonia release at low temperature. In addition, the calculated H_2 formation energy barriers, i.e., $[Al(NH_3)_6][Li_2(BH_4)_5] < [Al(NH_3)_6][BH_4]_3 < [Li(NH_3)][BH_4]$, are in agreement with the tendency of dehydrogenation temperatures determined experimentally. The incorporation of $[BH_4]^-$ into $[Al(NH_3)_6][BH_4]_3$ play an important role in decreasing the dehydrogenation temperature and improving the hydrogen purity of $[Al(NH_3)_6][Li_2(BH_4)_5]$.

KEYWORDS: Hydrogen storage; Density functional theory; Ammine metal borohydrides; Decomposition mechanism.

1. Introduction

Developing hydrogen storage materials with high gravimetric and desirable dehydrogenation temperature is one of the key challenges in using hydrogen as alternative energy source for mobile and stationary applications. [1-3] Over the past decades, many efforts have been devoted to developing materials with high hydrogen density and low dehydrogenation temperature. Metal borohydrides have received great attention because of their high gravimetric and volumetric densities. [4-9] However, many of the metal borohydrides either release hydrogen at high temperature or volatility and instability at room temperature, which make them unfavorable for practical application. For instance, $LiBH_4$ and $Ca(BH_4)_2$ start to release H_2 at temperature above 300 ^oC, and a complete dehydrogenation requires temperature higher than 500 ^oC. [8, 10] On the other hand, $Al(BH_4)_3$ is volatility at room temperature and releases by product of borane upon heating.[11]

It has been reported that combination of NH_3 into $M(BH_4)_n$ with the formation of ammine metal borohydrides (AMBs) is an effective strategy to improve thermo-dynamical stability of metal borohydride, and render dehydrogenation properties that comparable to that of amidoboranes and hydrazine borane. [12-21] However, many of the AMBs give rise to release undesirable gas of ammonia during decomposition. For instance, $LiBH_4 \cdot xNH_3$ and $Ca(BH_4)_2 \cdot nNH_3$ (n=1, 2 and 4) mainly release ammonia rather than hydrogen below 300 °C under dynamic situation. [13, 14, 22] Although $Al(BH_4)_3 \cdot 6NH_3$ mainly releases hydrogen upon heating, a certain amount of ammonia is still evolve along with hydrogen release.[12, 23] Recent studies indicate that the decomposition temperature of AMBs can be tuned extensively through combined metal cations with different ionicities/valences and NH_3/BH_4 ratio. [16, 23-25] Double-cation ammine borohydride, $[Al(NH_3)_6][Li_2(BH_4)_5]$, has been successfully synthesized through combination of $Al(BH_4)_3 \cdot 6NH_3$ and $LiBH_4$. $[Al(NH_3)_6][Li_2(BH_4)_5]$ shows significantly improve dehydrogenation properties over $LiBH_4 \cdot NH_3$ and $Al(BH_4)_3 \cdot 6NH_3$, with over 10 wt % of hydrogen released at temperature below 120 ^oC. [16]

The electronic structure and decomposition mechanisms of single metal cation AMBs have been studied by Density functional theory (DFT) calculation. [21, 25-27] Recent theoretic study indicates that the ammonia is weakly bound to the metal cations with low electronegativity (<1.2)

in AMBs, therefore tend to release ammonia at low temperature. In contrast, NH_3 is strongly coordinated with high electronegativity metal cations (>1.6), resulting in direct H_2 release in these materials. [27] Although this study has provided valuable insight of the decomposition processes of single metal cation AMBs, the results may not directly apply to double cations AMBs. For instance, the incorporation of $LiBH_4$ (with low electronegativity of 0.98 for Li cation) into $[Al(NH_3)_6][BH_4]_3$ with the formation of double cations ammine borohydride, $[Al(NH_3)_6][Li_2(BH_4)_5]$, not only results in reducing the dehydrogenation temperature but also improving the dehydrogenation purity. The strategy of using double-cations provides a feasible solution to advance the dehydrogenation properties of AMBs, however, the dehydrogenation mechanism is still unclear. Therefore, a detailed study of decomposition pathway will provide some insights for understanding the decomposition mechanisms of AMBs and thus to further improve their dehydrogenation performance.

Herein, the dehydrogenation mechanisms of $[Li(NH_3)][BH_4]$, $[Al(NH_3)_6][BH_4]_3$ and $[Al(NH_3)_6][Li_2(BH_4)_5]$ were studied by DFT calculation. Our calculated results show that the release of ammonia at low temperature for $[Li(NH_3)][BH_4]$ can be attributed to the low NH_3 vacancy formation energy and low NH_3 diffusion barrier. Both the $[Al(NH_3)_6][BH_4]_3$ and $[Al(NH_3)_6][Li_2(BH_4)_5]$ exhibit relatively high NH_3 vacancies formation energy and diffusion barriers. In addition, the $[Li(NH_3)][BH_4]$ shows the highest energy barrier of hydrogen formation among those three compounds; the calculated hydrogen formation energy barrier of $[Al(NH_3)_6][Li_2(BH_4)_5]$ is about 0.22 eV lower than that of $[Al(NH_3)_6][BH_4]_3$.

2. Computational method:

The crystal structures of $[Li(NH_3)][BH_4]$, $[Al(NH_3)_6][BH_4]_3$ and $[Al(NH_3)_6][Li_2(BH_4)_5]$ were taken from previous experimental results. Both the $[Li(NH_3)][BH_4]$ and $[Al(NH_3)_6][BH_4]_3$ crystallize in the orthorhombic structures with space groups *Pnma* and *Pbcn*, respectively; [13, 22, 23] while $[Al(NH_3)_6][Li_2(BH_4)_5]$ has a hexagonal structure with space group $P\bar{3}c1$. [16] The geometric structures of $[Li(NH_3)][BH_4]$, $[Al(NH_3)_6][BH_4]_3$ and $[Al(NH_3)_6][Li_2(BH_4)_5]$ were optimized by DFT calculation as implemented in MedeA@VASP code. [28] Exchange and correlation were treated in the generalized gradient approximation (GGA) of

Perdew-Burke-Ernzerhof (PBE). [29, 30] The electron-ion interactions were described by projector-augmented wave (PAW) approach, [31] treating $s^2s^1p^0$ of Li, s^2p^1 of B, s^2p^3 of N, s^2p^1 of Al and s^1p^0 for H as the explicit valence electrons. Plane waves with kinetic energy cutoff of 500 eV were used. The Brillouin zones were sampled by Monkhorst–Pack k-point meshes [32] for all compounds with meshes chosen to give a roughly constant density of k-points (30 Å) for all compounds. Structural relaxations of atomic positions were carried out until the residual forces were less than 0.02 $eV \cdot Å^{-1}$. To adapt the weak van der Waals interactions of dihydrogen bonds, the optB86b-vdW functional [33-35] was used for geometric optimization. For the calculation of NH_3 vacancies and H_2 formation energies, to prevent the spurious interactions between neighboring lattices and get well-converged results, 2 × 2 × 1 and 2 × 1 × 1 supercells of $[Li(NH_3)][BH_4]$ and $[Al(NH_3)_6][Li_2(BH_4)_5]$ were used. The NH_3 diffusion barriers and H_2 formation barriers were estimated by using climbing image nudged elastic band (CI-NEB) method. [36, 37]

3. Results and Discussion:

3.1 Bader charge

Table 1. Bader charges of $[Li(NH_3)][BH_4]$, $[Al(NH_3)_6][BH_4]_3$ and $[Al(NH_3)_6][Li_2(BH_4)_5]$.

Atom	Charge transfer		
	$[Li(NH_3)][BH_4]$	$[Al(NH_3)_6][BH_4]_3$	$[Al(NH_3)_6][Li_2(BH_4)_5]$
Li	0.8956	----	0.90
Al	----	2.43	2.43
B	1.64	1.64	1.62
N	-1.24	-1.32	-1.31
(N)H	0.40	0.42	0.43
(B)H	-0.65	-0.59	-0.63

To understand the decomposition mechanisms of $[Li(NH_3)][BH_4]$, $[Al(NH_3)_6][BH_4]_3$ and $[Al(NH_3)_6][Li_2(BH_4)_5]$, we first analyzed the charge transfer between the H, N, B atoms and metal cations (Li and Al). Table 1 shows the Bader charges[38] of H, N, B, Li and Al in $[Al(NH_3)_6][BH_4]_3$, $[Li(NH_3)][BH_4]$ and $[Al(NH_3)_6][Li_2(BH_4)_5]$. The charge transfers of Al, B, N

and H in $[Al(NH_3)_6][Li_2(BH_4)_5]$ are similar to that of $[Al(NH_3)_6][BH_4]_3$, and the charge transfer of Li in $[Al(NH_3)_6][Li_2(BH_4)_5]$ is similar to that of $[Li(NH_3)][BH_4]$. Therefore, the incorporation of $LiBH_4$ into $[Al(NH_3)_6][BH_4]_3$ barely affects the charge distribution in these compounds. Previous studies suggest that the Pauling electronegativity of metal cations and the specific geometry of the structure are two important factors for determining the charge distribution in the material. [26, 39, 40] Pauling electronegativity of Li and Al atoms are 0 .98 and 1.61, respectively. Incorporation of Li cations (low Pauling electronegativity) into $[Al(NH_3)_6][BH_4]_3$ has little effects of the charge distribution. For $[Al(NH_3)_6][BH_4]_3$ and $[Al(NH_3)_6][Li_2(BH_4)_5]$, the NH_3 units directly coordinate with Al atoms with Al-N bond lengths of 2.05 and 1.95 Å, respectively.[16, 23] The $LiBH_4$ molecules interact with $[Al(NH_3)_6][BH_4]_3$ molecules via $H^{+}\cdots\cdots{}^{-}H$ dihydrogen bonds for $[Al(NH_3)_6][Li_2(BH_4)_5]$. Hence, the improved dehydrogenation properties of $[Al(NH_3)_6][BH_4]_3$ through combination of $LiBH_4$ may be due to the specific geometry structure of $[Al(NH_3)_6][Li_2(BH_4)_5]$ rather than the charge distribution.

3.2 Formation and diffusion of ammonia vacancies

The previous experimental results demonstrated that $[Li(NH_3)][BH_4]$ tends to release a large amount of ammonia at temperature below 280 ^{o}C. [13] And $[Al(NH_3)_6][BH_4]_3$ releases 11.8 wt% of hydrogen (with a purity of 94.6 mol%) from room temperature to 300 ^{o}C. [12] The combination of $[Al(NH_3)_6][BH_4]_3$ and $LiBH_4$ with the formation of $[Al(NH_3)_6][Li_2(BH_4)_5]$ results in decrease of the dehydrogenation temperature and improvement of the hydrogen purity. [16] The transport properties of NH_3 are crucial to the kinetics of ammonia release from AMBs. Therefore, the microscopic mechanisms behind the release of ammonia may be relate to the formation and diffusivity of NH_3 vacancy. Hence, we calculated the formation energy of NH_3 vacancies using the following equation:

$$E_f = E_{total} - E(AMBs\text{-}NH_3) - E(NH_3)$$

Where E_{total} is the total energy of the AMBs supercells; $E(NH_3)$ represents the energy of isolate NH_3 molecule; $E(AMBs\text{-}NH_3)$ is the total energy of the AMBs supercells after NH_3 molecules are removed. The positive energy of E_f indicates that the formation of NH_3 vacancy is an endothermic process; while the negative energy of E_f indicates that the formation of NH_3 vacancy is an exothermic process.

Table 2. The NH_3 vacancies formation energies (E_f) and NH_3 diffusion barriers (E_b).

	$[Li(NH_3)][BH_4]$	$[Al(NH_3)_6][BH_4]_3$	$[Al(NH_3)_6][Li_2(BH_4)_5]$
E_f (eV)	1.13	1.67	1.69
E_b (eV)	0.30	1.56	1.42

As shown in Table 2, the calculated NH_3 vacancies formation energies are 1.13, 1.67 and 1.69 eV for $[Li(NH_3)][BH_4]$, $[Al(NH_3)_6][BH_4]_3$, and $[Al(NH_3)_6][Li_2(BH_4)_5]$, respectively. The relatively low NH_3 vacancy formation energy of $[Li(NH_3)][BH_4]$ suggests the weak coordination bond of Li-N, therefore the NH_3 vacancies can be formatted at relatively low temperature. The $[Al(NH_3)_6][BH_4]_3$, and $[Al(NH_3)_6][Li_2(BH_4)_5]$ show almost the same NH_3 formation energies, which can be attributed to the fact that NH_3 units coordinate with Al atom in both compounds. The bonding strength of Al-NH_3 bonds are mainly determined by Al cations, hence incorporation of $LiBH_4$ into $[Al(NH_3)_6][BH_4]_3$ does not appear to affect the Al-NH_3 bonds.

In addition to the formation energies of NH_3 vacancies, we further investigated the migration process of the NH_3, which involves mass transport and relates to the ammonia release. Although numerous diffusion pathways were examined, only the pathways with lowest energy barriers were described herein.

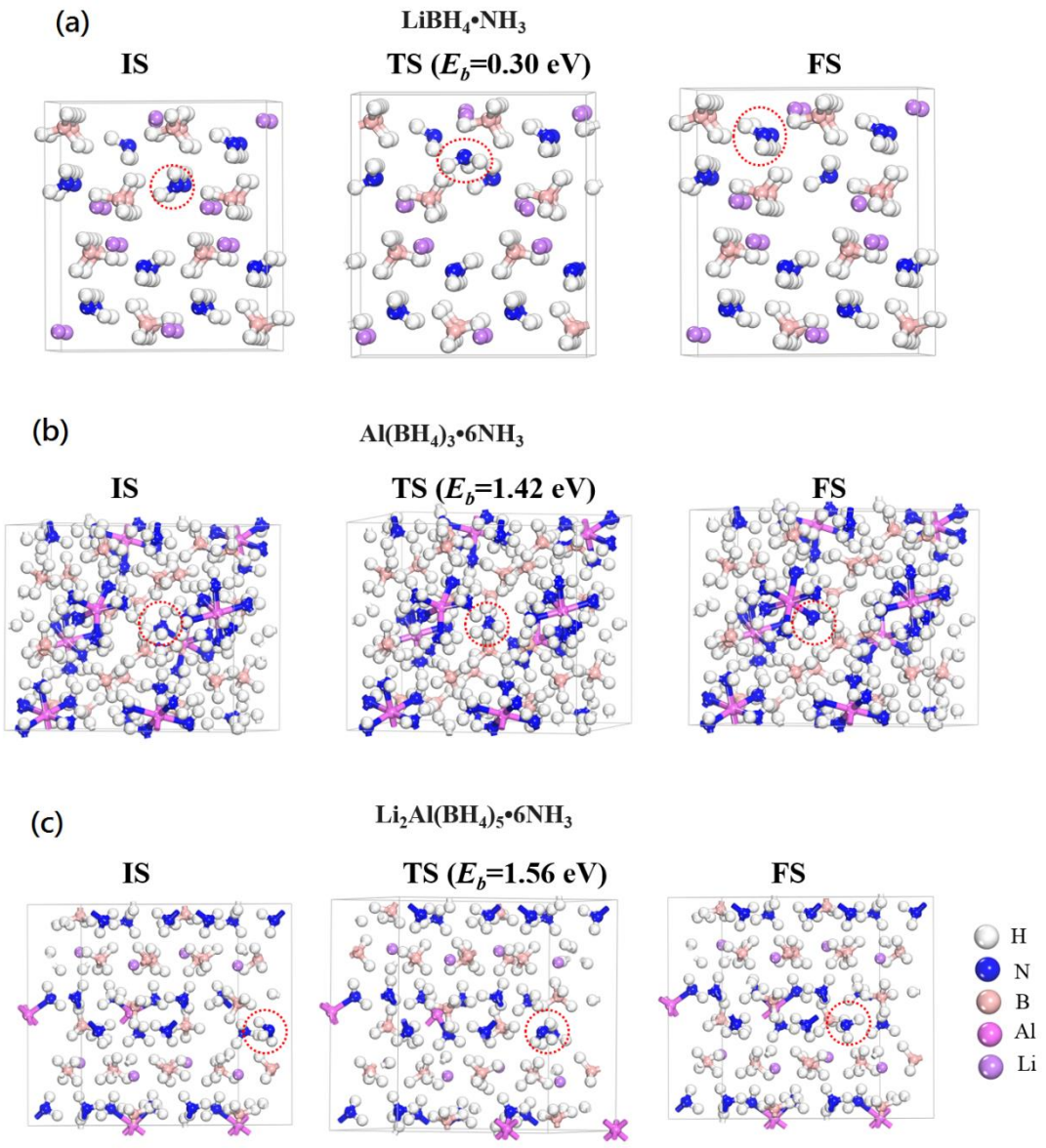

Figure 1. The initial (IS), transition (TS) and final (FS) geometric structure of NH_3 diffusion for (a) $[Li(NH_3)][BH_4]$, (b) $[Al(NH_3)_6][BH_4]_3$ and (c) $[Al(NH_3)_6][Li_2(BH_4)_5]$. E_b represents the calculated energy barrier.

As shown in Table 2 and Figure 1(a), the $[Li(NH_3)][BH_4]$ has a very low NH_3 diffusion barrier of 0.30 eV. This suggests that NH_3 would diffuse easily at low temperature, which is consistent with the experimental results that $[Li(NH_3)][BH_4]$ starts to release NH_3 at temperature below 100 ^oC. [13, 22] The low migration barrier for NH_3 in $[Li(NH_3)][BH_4]$ can be explained by the weak coordinate bonds of Li-NH_3. Previous report also suggested the weak coordinate bonds of Li-NH_3 and further combined $[Li(NH_3)][BH_4]$ with $MgCl_2$, $ZnCl_2$, and $AlCl_3$, all of which are able to

coordinate with ammonia to form stable ammonia metal complexes, can suppress the ammonia release. [13] Previous experimental results show that both $[Al(NH_3)_6][BH_4]_3$ and $[Al(NH_3)_6][Li_2(BH_4)_5]$ release hydrogen along with certain amount of ammonia. [12, 16] For instance, the dehydrogenation of $[Al(NH_3)_6][BH_4]_3$ accompany with the release of ammonia started at 150 ^oC, with a purity of 94.6 mol% from room temperature to 300 ^oC. [12] The hydrogen release of $[Al(NH_3)_6][Li_2(BH_4)_5]$ alone with the release of ammonia started at 125^oC with hydrogen purity of 97.0 mol % from room temperature to 300 ^oC. [16] In contrast to $[Li(NH_3)][BH_4]$, the calculated ammonia diffusion barriers are significantly high for $[Al(NH_3)_6][BH_4]_3$, and $[Al(NH_3)_6][Li_2(BH_4)_5]$, in agreement with experimental results that ammonia was released alone with hydrogen from these two compounds. [12, 16] Although the $[Al(NH_3)_6][Li_2(BH_4)_5]$ shows an improvement of hydrogen purity compared to that of $[Al(NH_3)_6][BH_4]_3$, the diffusion barrier of NH_3 vacancy in $[Al(NH_3)_6][Li_2(BH_4)_5]$ is slightly lower (0.14 eV) than that of $[Al(NH_3)_6][BH_4]_3$. The experimental results show that $[Al(NH_3)_6][BH_4]_3$ and $[Al(NH_3)_6][Li_2(BH_4)_5]$ start to release ammonia at temperature of 150 and 125 ^oC. Therefore, the release of ammonia from $[Al(NH_3)_6][BH_4]_3$ and $[Al(NH_3)_6][Li_2(BH_4)_5]$ may be not only depends on the NH_3 vacancies formation energies and diffusion barriers, but also relates to the hydrogen formation energies and barriers.

3.3 Hydrogen formation energies and barriers

Table 3. The formation energies and barriers of H_2 release via (N)H and (B)H combination by using crystal model ($E_{H2\text{-}C}$) and molecule model ($E_{H2\text{-}M}$).

	$[Li(NH_3)][BH_4]$	$[Al(NH_3)_6][BH_4]_3$	$[Al(NH_3)_6][Li_2(BH_4)_5]$
$E_{H2\text{-}C}$ (eV)	0.77	0.01	0.24
$E_{H2\text{-}M}$ (eV)	-0.02	-0.29	-0.38
E_b (eV)	2.06	1.76	1.54

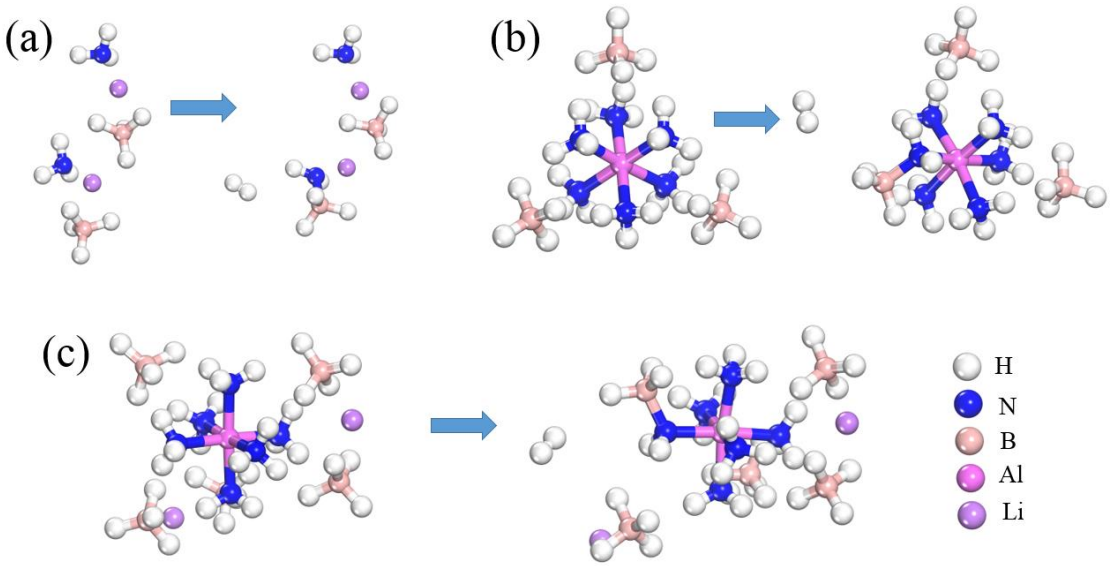

Figure 2. The initial and final geometry structure of hydrogen release from (a) $[Li(NH_3)][BH_4]$, (b) $[Al(NH_3)_6][BH_4]_3$ and (c) $[Al(NH_3)_6][Li_2(BH_4)_5]$.

Our previous studies suggest that dehydrogenation of AMBs is achieved by the dissociation of a H atom from NH_3 (represent as (N)H) and a H atom from $[BH_4]^-$ (represent as (B)H). [41, 42] Hence, we further calculated the H_2 formation energies by moving one (N)H and one (B)H atom away from host N or B atom to form a hydrogen molecule with H-H distance of 0.74 Å in the supercell of AMBs. The geometry optimization was first performed by fixed the H_2 positions and relaxed the rest of the atoms, following by full relaxed all of the atoms in the supercell. As discuss in our previous studies, the formation of H_2 molecules lead to significant rearrangement of the surrounding lattice, which results in overestimated hydrogen formation energies. [41, 42] Therefore, we further calculated the hydrogen formation energies by using the molecule model in which two formula units of $[Li(NH_3)][BH_4]$, and one formula unit of $[Al(NH_3)_6][BH_4]_3$ and $[Al(NH_3)_6][Li_2(BH_4)_5]$ were placed in a cubic cell with lattice parameter of 20 Å.

As shown in Table 3, the calculated hydrogen formation energies by using supercell of AMBs are 0.77, 0.01 and 0.24 eV for $[Li(NH_3)][BH_4]$, $[Al(NH_3)_6][BH_4]_3$, and $[Al(NH_3)_6][Li_2(BH_4)_5]$, respectively. In consistent with our previous theoretical study, the dissociation of H_2 results in dramatic distort of lattices. The hydrogen formation energies calculated by molecule model are -0.02, -0.29 and -0.38 eV for $[Li(NH_3)][BH_4]$, $[Al(NH_3)_6][BH_4]_3$, and $[Al(NH_3)_6][Li_2(BH_4)_5]$, respectively. The calculated negative hydrogen formation energies indicate that the release of

hydrogen from $[Al(NH_3)_6][BH_4]_3$ and $[Al(NH_3)_6][Li_2(BH_4)_5]$ are exothermic processes, in agreement with experimental observation. [12, 16]

As shown in Figure 2, for all the three compounds, the combination of the (N)H and (B)H lead to rearrangement of the surrounding atoms. Generally, the $[NH_2]^-$ and BH_3 units reoriented and BH_3 units moved toward $[NH_2]^-$ with the formation of NH_2-BH_3 complexes. The N-B distances reduce to 1.58 Å, indicating the formation of N-B bonds. The Al-N bond lengths range from 1.98 to 2.05 Å after structural rearrangements. As reported in previous literatures, the molecular complex $[Al(NH_3BH_3)(BH_4)_3]$ and $Na[Al(NH_2BH_3)_4]$ demonstrates favorable dehydrogenation properties with high purity of hydrogen release. [43-45] In the case of $Na[Al(NH_2BH_3)_4]$, the Al-N bond lengths range from 1.84 to 1.93 Å, [43] which are slightly shorter than that of $[Al(NH_3)_6][BH_4]_3$ and $[Al(NH_3)_6][Li_2(BH_4)_5]$ after structural rearrangements. The potential formation of $[Al(NH_2BH_3)_4]^-$ or $[Al(NH_3BH_3)(BH_4)_3]$-like complexes from $[Al(NH_3)_6][BH_4]_3$ and $[Al(NH_3)_6][Li_2(BH_4)_5]$ may play an important role for the high purity hydrogen release.

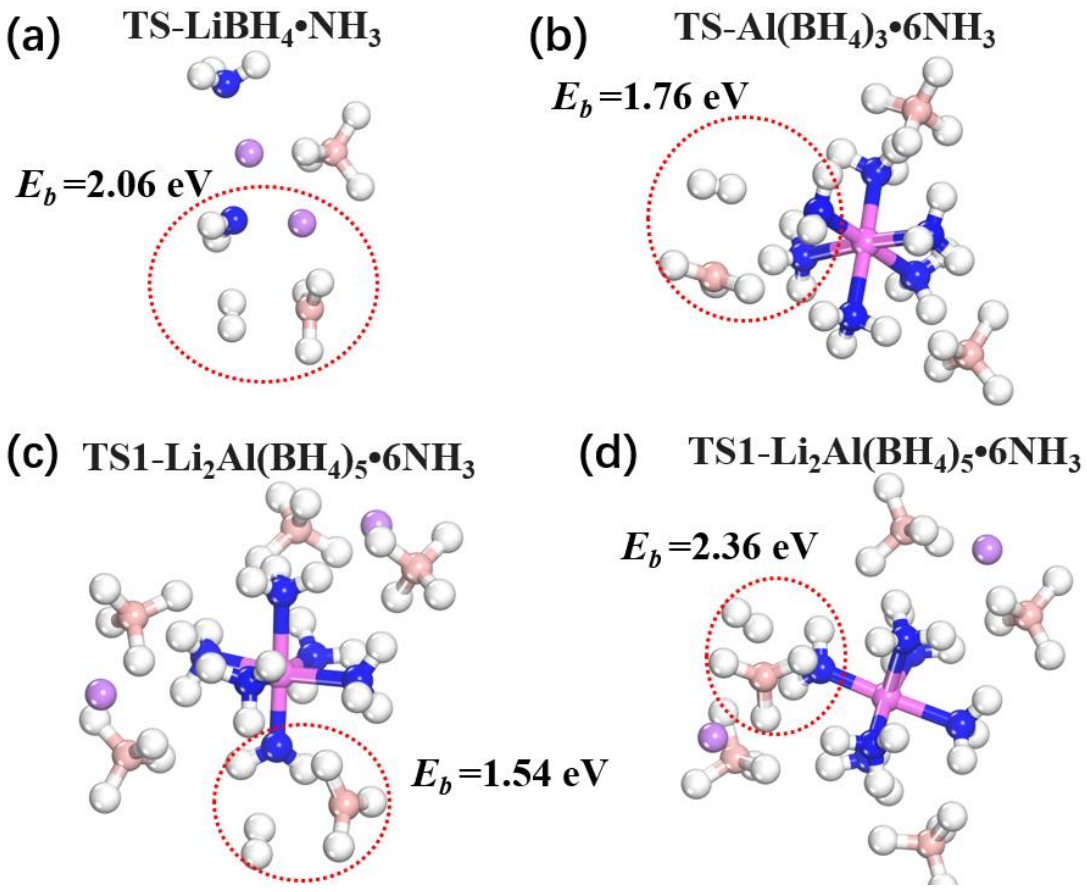

Figure 3. The transition geometric structures and energy barriers of hydrogen release from (a) $[Li(NH_3)][BH_4]$, (b) $[Al(NH_3)_6][BH_4]_3$ and (c) $[Al(NH_3)_6][Li_2(BH_4)_5]$. E_b represent the calculated energy barriers.

Since the hydrogen formation energies calculated from crystal model have been overestimated, the energy barriers of H_2 formation were calculated from molecule model. As shown in Tabel 3 and Figure 3, the energy barrier of H_2 formation from $[Li(NH_3)][BH_4]$ is 2.06 eV, the high energy barrier indicates that hydrogen release via (N)H and (B)H combination would occur at high temperature. As discussed above, the formation energy and diffusion barrier of NH_3 vacancy are 1.13 eV and 0.30 eV, which are significantly lower than the H_2 formation barrier for $[Li(NH_3)][BH_4]$. Therefore, ammonia would release from $[Li(NH_3)][BH_4]$ at a low temperature before H_2 release, which is consistent with the experimental results that $[Li(NH_3)][BH_4]$ mainly release NH_3 rather than H_2 at temperature below 280 ^oC. [13, 22] The transition geometric structure of hydrogen release from $[Li(NH_3)][BH_4]$ (Figure 3(a)) shows the broken of B-H and N-H bonds with the formation of H_2 molecule. The H_2 molecule is located between $[NH_2]^-$ and BH_3 units with H_2-$[NH_2]^-$ and H_2-BH_3 distances of 2.50 and 2.66 Å, respectively. Both N-H and B-H bonds broken in the transition state, unlike that in the transition state of $[NH_3BH_3]_2$ where the N-H and B-H distances stretched to 1.37 and 1.36 Å, respectively. [46] Meanwhile, the Li atom and $[NH_2]^-$ move around each other and lead to slightly reduce the Li-N distance from 2.07 to 1.93 Å due to the coulombian interaction between Al cation and $[NH_2]^-$.

The experimental results suggest that $[Li(NH_3)][BH_4]$ and $[Al(NH_3)_6][BH_4]_3$ starts to release H_2 at temperature around 300 and 100 ^oC, respectively.[12, 13] Compared to that of $[Li(NH_3)][BH_4]$, $[Al(NH_3)_6][BH_4]_3$ has relatively high NH_3 vacancy formation energy and NH_3 diffusion barrier, which would prevent NH_3 release at low temperature; in addition, the lower hydrogen formation energy barrier (0.3 eV lower) leads to lower dehydrogenation temperature of $[Al(NH_3)_6][BH_4]_3$. The transition geometric structure of $[Al(NH_3)_6][BH_4]_3$ (Figure 3(b)) shows that the H_2 molecule is located between $[NH_2]^-$ and BH_3 unit. The shortest H_2-$[NH_2]^-$ and H_2-BH_3 distances are 2.36 and 2.35 Å, respectively, which are slightly shorter than that in the transition

state of $[Li(NH_3)][BH_4]$. In addition, the $[NH_2]^-$ shortening its distance to the Al cation from 2.02 to 1.87 Å due to the coulombian interaction between Al cation and $[NH_2]^-$.

The calculated H_2 formation energy barrier of $[Al(NH_3)_6][Li_2(BH_4)_5]$ is 1.54 eV (pathway 1, Figure 3 (c)), which is 0.22 eV lower than that of $[Al(NH_3)_6][BH_4]_3$. The H_2 formation energy barrier would result in lower dehydrogenation temperature, in good agreement with experimental result. [16] Similar to that of $[Li(NH_3)][BH_4]$ and $[Al(NH_3)_6][BH_4]_3$, the formation H_2 molecule was located between $[NH_2]^-$ and BH_3 with shortest H_2-$[NH_2]^-$ and H_2-BH_3 distances of 2.53 and 2.51 Å, respectively. The release of hydrogen from $[Al(NH_3)_6][BH_4]_3$ and $[Al(NH_3)_6][Li_2(BH_4)_5]$ is not only involved the broken of N-H and B-H bonds but also lead to rotation of NH_3 units around Al cation and broken of neighboring dihydrogen bonds. For $[Al(NH_3)_6][Li_2(BH_4)_5]$, the two addition $[BH_4]^-$ surround $[Al(NH_3)_6][BH_4]_3$ would adjust to form dihydrogen bonds during the hydrogen release process, resulting in lower dehydrogenation barrier compared to that of $[Al(NH_3)_6][BH_4]_3$. Therefore, introduction of addition $[BH_4]^-$ into $[Al(NH_3)_6][BH_4]_3$ is an effective way to reduce the dehydrogenation temperature. We further calculated dehydrogenation pathway 2 in which hydrogen released via combination of (B)H from $LiBH_4$ and (N)H from $[Al(NH_3)_6][BH_4]_3$. As shown in Figure 3(d), the calculated energy barrier is 2.36 eV, which is 0.6 eV higher than that of $[Al(NH_3)_6][BH_4]_3$. The combination of (B)H from $LiBH_4$ and (N)H from $[Al(NH_3)_6][BH_4]_3$ results in significant movement of Li atoms, which lead to increase the H_2 formation barrier. The calculated H_2 formation barriers of pathway 1 is significantly lower than that of pathway 2, indicating that a direct elimination of H_2 through pathway 2 is not competitive. Although Li cation didn't directly involve in the above dehydrogenation process, it should be noted that Li transfers it electron to the surrounding (B)H atoms. Further experimental and theoretical study is required to understand to role of metal cations in the dehydrogenation process of double cation ammine metal borohydrides.

Over all, the above calculations show the tendency of hydrogen formation barrier, i.e., $[Al(NH_3)_6][Li_2(BH_4)_5] < [Al(NH_3)_6][BH_4]_3 < [Li(NH_3)][BH_4]$. Compared to that of $[Al(NH_3)_6][BH_4]_3$, the two addition $[BH_4]^-$ in $[Al(NH_3)_6][Li_2(BH_4)_5]$ adjust to form dihydrogen bonds with neighboring NH_3 units during dehydrogenation process, which renders a lower hydrogen formation barrier.

4. Conclusions

Density functional theory have been employed to investigate the decomposition processes of $[Li(NH_3)][BH_4]$, $[Al(NH_3)_6][BH_4]_3$ and $[Al(NH_3)_6][Li_2(BH_4)_5]$. Compared to that of $LiBH_4$ and $[Al(NH_3)_6][BH_4]_3$, the combination of $LiBH_4$ and $[Al(NH_3)_6][BH_4]_3$ with the formation of $[Al(NH_3)_6][Li_2(BH_4)_5]$ does not appear to affect the charge distribution. The $[Li(NH_3)][BH_4]$ shows low NH_3 vacancy formation energy and diffusion barrier, which explain the experimental results that ammonia release from $[Li(NH_3)][BH_4]$ at low temperature. Both $[Al(NH_3)_6][BH_4]_3$ and $[Al(NH_3)_6][Li_2(BH_4)_5]$ show relatively high NH_3 vacancy formation energies and diffusion barriers, which suppress ammonia release before dehydrogenation. In addition, the calculated H_2 formation energy barriers of $[Al(NH_3)_6][Li_2(BH_4)_5]$, $[Al(NH_3)_6][BH_4]_3$ and $[Li(NH_3)][BH_4]$ are 1.54, 1.76 and 2.06 eV, respectively, in agreement with the tendency of dehydrogenation temperatures determined experimentally, i.e., $[Al(NH_3)_6][Li_2(BH_4)_5] < [Al(NH_3)_6][BH_4]_3 < [Li(NH_3)][BH_4]$.

ACKNOWLEDGEMENTS

This work is supported by the National Science Fund for Distinguished Young Scholars (51625102), National Natural Science Foundation of China (11074099, 51601068) and Natural Science Foundation of Fujian Province (2016J05129).

REFERENCES

[1] Chen P, Xiong ZT, Luo JZ, Lin JY, Tan KL. Interaction of hydrogen with metal nitrides and imides. Nature. 2002;420:302-4.

[2] Schlapbach L, Züttel A. Hydrogen-storage materials for mobile applications. Nature. 2001;414:353-8.

[3] Durbin DJ, Malardier-Jugroot C. Review of hydrogen storage techniques for on board vehicle applications. Int J Hydrogen Energy. 2013;38:14595-617.

[4] Miwa K, Aoki M, Noritake T, Ohba N, Nakamori Y, Towata S-i, et al. Thermodynamical

stability of calcium borohydride $Ca(BH_4)_2$. Phys Rev B. 2006;74:155122.

[5] Paskevicius M, Jepsen LH, Schouwink P, Cerny R, Ravnsbaek DB, Filinchuk Y, et al. Metal borohydrides and derivatives - synthesis, structure and properties. Chem Soc Rev. 2017;46:1565-634.

[6] Humphries TD, Kalantzopoulos GN, Llamas-Jansa I, Olsen JE, Hauback BC. Reversible hydrogenation studies of $NaBH_4$ milled with Ni-containing additives. J Phys Chem C. 2013;117:6060-5.

[7] Saldan I, Hino S, Humphries TD, Zavorotynska O, Chong M, Jensen CM, et al. Structural changes observed during the reversible hydrogenation of $Mg(BH_4)_2$ with Ni-based additives. J Phys Chem C. 2014;118:23376-84.

[8] Li H-W, Yan Y, Orimo S-i, Züttel A, Jensen CM. Recent progress in metal borohydrides for hydrogen storage. Energies. 2011;4:185-214.

[9] George L, Saxena SK. Structural stability of metal hydrides, alanates and borohydrides of alkali and alkali-earth elements: a review. Int J Hydrogen Energy. 2010;35:5454-70.

[10] Yan Y, Remhof A, Hwang S, Li H, Mauron P, Orimo S, et al. Pressure and temperature dependence of the decomposition pathway of $LiBH_4$. Phys. Chem. Chem. Phys.. 2012;14:6514-9.

[11] Nakamori Y, Li HW, Matsuo M, Miwa K, Towata S, Orimo S. Development of metal borohydrides for hydrogen storage. J Phys Chem Solids. 2008;69:2292-6.

[12] Guo YH, Yu XB, Sun WW, Sun DL, Yang WN. The hydrogen‐enriched Al–B–N system as an advanced solid hydrogen‐storage candidate. Angew Chem. 2011;123:1119-23.

[13] Guo YH, Xia GL, Zhu Y, Gao L, Yu XB. Hydrogen release from amminelithium borohydride, $LiBH_4 \cdot NH_3$. Chem. Commun. 2010;46:2599-601.

[14] Chu H, Wu G, Xiong Z, Guo J, He T, Chen P. Structure and hydrogen storage properties of calcium borohydride diammoniate. Chem Mater. 2010;22:6021–8.

[15] Soloveichik G, Her JH, Stephens PW, Gao Y, Rijssenbeek J, Andrus M, et al. Ammine magnesium borohydride complex as a new material for hydrogen storage: structure and properties of $Mg(BH_4)_2 \cdot 2NH_3$. Inorg Chem. 2008;47:4290-8.

[16] Guo YH, Wu H, Zhou W, Yu XB. Dehydrogenation tuning of ammine borohydrides using double-metal cations. J Am Chem Soc. 2011;133:4690–3.

[17] Jepsen LH, Ley MB, Cerný R, Lee Y, Cho YW, Ravnsbaek DB, et al. Trends in syntheses, structures, and properties for three series of ammine rare-earth metal borohydrides, $M(BH_4)_3 \cdot nNH_3$ (M = Y, Gd, and Dy). Inorg Chem. 2015;54:7402-14.

[18] Huang JM, Ouyang LZ, Gu QF, Yu XB, Zhu M. Metal-borohydride-modified $Zr(BH_4)_4 \bullet 8NH_3$: low-temperature dehydrogenation yielding highly pure hydrogen. Chem-Eur J. 2015;21:14931-6.

[19] Yang YJ, Liu YF, Li Y, Gao MX, Pan HG. Fluorine-substituted $Mg(BH_4)_2 \bullet 2NH_3$ with improved dehydrogenation properties for hydrogen storage. J Mater Chem A. 2015;3:570-8.

[20] Stennett TE, Harder S. s-Block amidoboranes: syntheses, structures, reactivity and applications. Chem Soc Rev. 2016;45:1112-28.

[21] Moury R, Demirci U. Hydrazine borane and hydrazinidoboranes as chemical hydrogen storage materials. Energies. 2015;8:3118.

[22] Johnson SR, David WIF, Royse DM, Sommariva M, Tang CY, Fabbiani F, et al. The monoammoniate of lithium borohydride, $Li(NH_3)BH_4$: an effective ammonia storage compound. Chem -An Asian Journal. 2009;4:849-54.

[23] Tang Z, Tan Y, Wu H, Gu Q, Zhou W, Jensen CM, et al. Metal cation-promoted hydrogen generation in activated aluminium borohydride ammoniates. Acta Mater. 2013;61:4787-96.

[24] Chen X, Yuan F, Gu Q, Tan Y, Liu H, Dou S, et al. Improved dehydrogenation properties of the combined $Mg(BH_4)_2 \cdot 6NH_3$–nNH_3BH_3 system. Int J Hydrogen Energy. 2013;38:16199-207.

[25] Emdadi A, Demir S, Kışlak Y, Tekin A. Computational screening of dual-cation metal ammine borohydrides by density functional theory. J Phys Chem C. 2016;120:13340-50.

[26] Wang K, Zhang J-G, Jiao J-S, Zhang T, Zhou Z-N. A First-principles study: structure and decomposition of mono-/bimetallic ammine borohydrides. J Phys Chem C. 2014;118:8271-9.

[27] Welchman E, Thonhauser T. Decomposition mechanisms in metal borohydrides and their ammoniates. J Mater Chem A. 2017;5:4084-92.

[28] Kresse G, Furthmüller J. Efficient iterative schemes for ab initio total-energy calculations using a plane-wave basis set. Phys Rev B. 1996;54:11169.

[29] Perdew JP, Burke K, Ernzerhof M. Generalized gradient approximation made simple. Phys Rev Lett. 1996;77:3865-8.

[30] Perdew JP, Burke K, Wang Y. Generalized gradient approximation for the

exchange-correlation hole of a many-electron system. Phys Rev B. 1996;54:16533-9.

[31] Blöchl PE. Projector augmented-wave method. Phys Rev B. 1994;50:17953.

[32] Monkhorst HJ, Pack JD. Special points for Brillouin-zone integrations. Phys Rev B. 1976;13:5188-92.

[33] Klimes J, Bowler DR, Michaelides A. Van der Waals density functionals applied to solids. Phys Rev B. 2011;83.

[34] Klimes J, Bowler DR, Michaelides A. Chemical accuracy for the van der Waals density functional. J Phys: Condens Matter. 2009;22:022201.

[35] Dion M, Rydberg H, Schroder E, Langreth DC, Lundqvist BI. Van der Waals density functional for general geometries. Phys Rev Lett. 2004;92:246401.

[36] Henkelman G, Uberuaga BP, Jónsson H. A climbing image nudged elastic band method for finding saddle points and minimum energy paths. J Chem Phy. 2000;113:9901-4.

[37] Henkelman G, Jónsson H. Improved tangent estimate in the nudged elastic band method for finding minimum energy paths and saddle points. J Chem Phys. 2000;113:9978-85.

[38] Henkelman G, Arnaldsson A, Jónsson H. A fast and robust algorithm for Bader decomposition of charge density. Comput Mater Sci. 2006;36:254-360.

[39] Roedern E, Jensen TR. Ammine-stabilized transition-metal borohydrides of iron, cobalt, and chromium: synthesis and characterization. Inorg Chem. 2015;54:10477-82.

[40] Staubitz A, Robertson APM, Manners I. Ammonia-borane and related compounds as dihydrogen sources. Chem Rev. 2010;110:4079-124.

[41] Chen XW, Yuan F, Tan YB, Tang ZW, Yu XB. Improved dehydrogenation properties of $Ca(BH_4)_2{\cdot}NH_3$ (n=1, 2, and 4) combined with $Mg(BH_4)_2$. J Phys Chem C. 2012;116:21162-8.

[42] Chen XW, Yu XB. Electronic structure and initial dehydrogenation mechanism of $M(BH_4)_2{\cdot}2NH_3$ (M = Mg, Ca, and Zn): A First-principles investigation. J Phys Chem C. 2012;116:11900-6.

[43] Dovgaliuk I, Jepsen LH, Safin DA, Łodziana Z, Dyadkin VA, Jensen TR, et al. a composite of complex and chemical hydrides yields the first Al−based amidoborane with improved hydrogen storage properties. Chem-Eur J. 2015;21:14562-70.

[44] Dovgaliuk I, Duff CSL, Robeyns K, Devillers M, Filinchuk Y. Mild dehydrogenation of

ammonia borane complexed with aluminum borohydride. Chem Mater. 2015;25:768-77.

[45] Dovgaliuk I, Filinchuk Y. Aluminium complexes of B- and N-based hydrides: synthesis, structures and hydrogen storage properties. Int J Hydrogen Energy. 2016;41:15489-504.

[46] Nguyen MT, Nguyen VS, Matus MH, Gopakumar G, Dixon DA. Molecular mechanism for H_2 release from BH_3NH_3, including the catalytic role of the lewis acid BH_3. J. Phys. Chem. A. 2007;111:679-90.